COBEM2015

ABCM Associação Brasileira de Engenharia e Ciências Mecânicas

23rd ABCM International Congress of Mechanical Engineering
December 6-11, 2015, Rio de Janeiro, RJ, Brazil

LAMINAR AND TURBULENT NATURAL CONVECTION IN 2D-SQUARE CAVITIES

José Renê de Sousa Rocha
Rebeca P. Marcondes
Ivens da Costa Menezes Lima
Francisco Marcondes
Department of Metallurgical Engineering and Material Science, Federal University of Ceará, Pici Campus, Block 714, Fortaleza, Ceará 60455-760, Brazil
renner.91@hotmail.com, rebecapereiramarc@hotmail.com, ivenscml@yahoo.com.br, marcondes@ufc.br

Abstract. *Laminar and turbulent natural convection in cavities has several important applications in the industry, such as cooling of microelectronic circuits, fire control, thermal isolation, solar collectors, flow in nuclear reactors, among them. The knowledge of the most important factors that control the flow inside a cavity is crucial to the design and analysis of equipment in which the physical processes are governed by natural convection. In the present study, the laminar and turbulent regimes for a two-dimensional square cavity are investigated by changing the Rayleigh number. The ANSYS CFX® software was used to perform the numerical investigation. The $k-\omega$ turbulence model was used to model the turbulent regime. All the simulations were performed using a two-dimensional square cavity with two adiabatic walls, a heated and a cooled wall, both with uniform temperature profile. The results, for a Prandtl number equal to* 0.71*, were presented in terms of isotherms, streamlines, local and average Nusselt number along the heated wall. The obtained results were in a good agreement with the ones presented in the literature.*

Keywords: *Natural convection, $k-\omega$ turbulence model, EbFVM, ANSYS CFX®*

1. INTRODUCTION

The study of the natural convection phenomenon in square cavities has been studied by many researchers due to its various applications in engineering such as cooling of electric components, cooling in nuclear reactors, solar collectors and combustion processes. This type of problem has been thoroughly investigated through numerical, analytical and experimental procedures. Nonetheless there are still some problems that need to be understood, especially, in turbulent flows.

Lankhorst (1991) studied laminar and turbulent regimes in cavities filled with both air and water, with Rayleigh Ra numbers ranging from 10^1 to 10^{12} using the Lam and Bremhorst (1981) $k-\epsilon$ turbulence model. Sharif and Liu (2003) conducted numerical experiments, using air as a fluid material, for $Ra = 4.9 \times 10^{10}$ under the same cavity settings but comparing the performance of the $k-\epsilon$ and Wilcox (1986) $k-\omega$ models. The introduction of the buoyancy turbulent production term was analyzed by Rundle and Lightstone (2007) under the previously cited turbulence models and the Shear Stress Model (SST) model; the results showed that the $k-\omega$ model has more accuracy for this type of simulation and that the buoyancy turbulence production terms do not increase the accuracy of the simulation and therefore does not need to be included.

Vieira (2010) used ANSYS CFX® as a tool to evaluate the influence of the boundary conditions, geometries and properties of the fluid and mainly the volumetric heat generation rate due to nuclear fission of the fluid, for different Prandtl (Pr) and Rayleigh numbers for 2D square and semicircular cavities.

Researchers have recently studied several parameters that affect the fluid pattern inside confined cavities, such as aspect ratio (Trias *et al.*, 2007) and different geometries, for example retangular shapes (Ganguli *et al.*, 2009) , triangular configurations (Basak *et al.*, 2009) and trapezoidal (Silva *et al.*, 2012; Fontana *et al.*, 2010) cavities.

The present work focuses on the Ra number influence for both flow and heat transfer using air ($Pr = 0.7$) as working fluid for laminar and turbulent regimes in a square cavity, where the vertical walls are differently heated and the top and bottom walls are adiabatic. The results are shown in terms of isotherms, streamlines, local and average Nu numbers.

2. MATHEMATICAL FORMULATION

Figure 1 shows the cavity and one grid configuration employed for the numerical simulations. The vertical left and right walls of the square cavity are heated and cooled, respectively, at constant temperatures T_h and T_c, where $T_h > T_c$ while the horizontal walls remain adiabatic. The general schematic configuration of the two-dimensional square cavity

filled with air is shown in Fig. 2 along with the coordinates.

In this work is considered that the fluid properties were constant, except by the buoyancy term along the y-direction in the Navier-Strokes equations. Incompressible fluid flow and thermal radiation effects were neglected in the 2D equation for laminar and turbulent flows. Moreover, the turbulent problems were solved with the $k-\omega$ equations, which assumes that the turbulent viscosity μ_t is related to the turbulent kinetic energy k and the turbulent frequency ω. The mathematical solution is given by Equations 1 through 8.

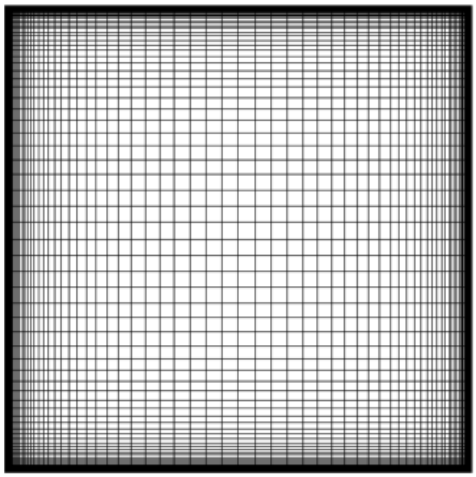

Figure 1: Mesh with grid refinement 80×80

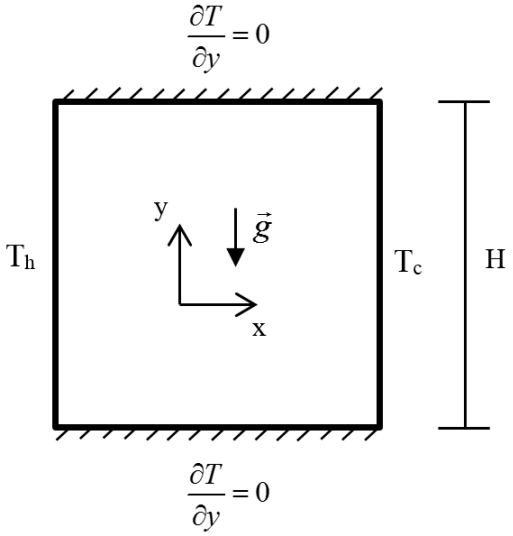

Figure 2: General schematic configuration

$$\frac{\partial \rho}{\partial t} + \frac{\partial}{\partial x_j}(\rho U_j) = 0 \tag{1}$$

$$\frac{\partial \rho U_i}{\partial t} + \frac{\partial}{\partial x_j}(\rho U_i U_j) = -\frac{\partial p'}{\partial x_i} + \frac{\partial}{\partial x_j}\left[\mu_{eff}\left(\frac{\partial U_i}{\partial x_j} + \frac{\partial U_j}{\partial x_i}\right)\right] + S_M \tag{2}$$

$$\frac{\partial T}{\partial t} + \frac{\partial U_j T}{\partial x_j} = \frac{\partial}{\partial x_j}\left[\left(\frac{\nu}{Pr} + \frac{\nu_t}{\sigma_t}\right)\frac{\partial T}{\partial x_j}\right] \tag{3}$$

$$\frac{\partial \rho k}{\partial t} + \frac{\partial}{\partial x_j}(\rho U_j k) = \frac{\partial}{\partial x_j}\left[\left(\mu + \frac{\mu_t}{\sigma_k}\right)\frac{\partial k}{\partial x_j}\right] + P_k - \beta' \rho k \omega \tag{4}$$

$$\frac{\partial \rho \omega}{\partial t} + \frac{\partial}{\partial x_j}(\rho U_j \omega) = \frac{\partial}{\partial x_j}\left[\left(\mu + \frac{\mu_t}{\sigma_\omega}\right)\frac{\partial \omega}{\partial x_j}\right] + \alpha \frac{\omega}{k} P_k - \beta \rho \omega^2 \tag{5}$$

$$P_k = \mu_t\left(\frac{\partial U_i}{\partial x_j} + \frac{\partial U_j}{\partial x_i}\right)\frac{\partial U_i}{\partial x_j} - \frac{2}{3}\frac{\partial U_k}{\partial x_k}\left(3\mu_t \frac{\partial U_k}{\partial x_k} + \rho k\right) \tag{6}$$

$$\mu_t = \rho \frac{k}{\omega} \tag{7}$$

$$p' = p + \frac{2}{3}\rho k \tag{8}$$

In the above equations U_i are the velocities components (m/s), ρ (kg/m^3) is the fluid density, T is the fluid temperature (K), p' is the modified pressure (Pa), P_k is the turbulence production rate $(kg/m \cdot s^3)$, σ_t is the turbulent Prandtl number (0.9), ν is the kinematic viscosity (m^2/s), ν_t is the kinematic turbulent viscosity (m^2/s), μ is the dynamic viscosity $(kg/m \cdot s)$, k is the kinetic turbulent energy (m^2/s^2), ω is the turbulent dissipation rate (m^2/s^2), μ_t is the turbulent viscosity $(kg/m \cdot s)$ and $\mu_{eff} = \mu + \mu_t$ (if the flow is laminar $\mu_t = 0$) . The momentum source S_M along the y-axis is given by $\mathcal{S}_M = -g\beta(T - T_0)$, where T_0 is the reference temperature, g is the gravitational acceleration (m/s^2) and β is the thermal expansion coefficient of air $(1/K)$.

The $k-\omega$ model constants are given by

$$\beta' = 0.09 \tag{9}$$
$$\alpha = 5/9 \tag{10}$$
$$\beta = 0.075 \tag{11}$$
$$\sigma_k = 2 \tag{12}$$
$$\sigma_\omega = 2 \tag{13}$$

The boundary conditions for the vertical walls are given by

$$T(x=0,y) = T_h \qquad u(x=0,y) = v(x=0,y) = 0 \tag{14}$$
$$T(x=H,y) = T_c \qquad u(x=H,y) = v(x=H,y) = 0 \tag{15}$$
$$\left.\frac{\partial T}{\partial y}\right)_{y=0} = 0 \qquad u(x,y=0) = v(x,y=0) = 0 \tag{16}$$
$$\left.\frac{\partial T}{\partial y}\right)_{y=H} = 0 \qquad u(x,y=H) = v(x,y=H) = 0 \tag{17}$$

The boundary conditions used to solve the equations for k and ω were provided by the automatic near wall treatment, which automatically switch from wall functions to a low-Reynolds near wall formulation as the mesh is refined.

If the set of eqs. (1) to (3) are written in a dimensionless form, it can be shown that they are function of the Ra and Pr numbers, where the Ra number is given by

$$Ra = \frac{g\beta\left(T_h - T_c\right)H^3}{\nu\alpha} \tag{18}$$

where T_h denotes the temperature in the heated wall, T_c is the temperature in the cooled wall and Pr is 0.71 for all the cases.

3. RESULTS AND DISCUSSION

This section is divided into three parts and presents the results in terms of isotherms, local Nusselt number Nu and average Nusselt number $\overline{Nu}$. Presented first is the mesh refinement study, then the results of isotherms ranging from $Ra = 10^3$ to 10^8. Finally, the solution for two turbulent flows are presented in terms of local and average Nusselt Numbers. The benchmarks solutions available in the literature for these two case studies are also presented. For laminar flow ($10^3 \leq Ra \leq 10^8$), the solution was considered to reach steady state regime when the error for mass, momentum. and energy equation was smaller than 10^{-7}. A similar criteria was used to the turbulent flow, but the tolerance was increased to 10^{-6}, due to convergence problems.

3.1 Mesh refinement study

Mesh refinement study was performed for all simulations and the results were considered mesh independent when the $\overline{Nu}$ presented an error less then 0.1%. The Nu and $\overline{Nu}$ were defined by

$$Nu = \frac{\left.-\frac{\partial T}{\partial x}\right)_{x=0}}{(T_h - T_c)/Y} \tag{19}$$
$$\overline{Nu} = \frac{1}{H}\int_0^H Nu\, dy \tag{20}$$

where H denotes the height of the heated wall and y denotes the coordinates along y-axis.

The refinement was mainly focused at the vertical walls where the gradients were expected to be higher. Non-uniform and structured grids of 60×60, 80×80, 100×100, 120×120, 140×140, 160×160 were used. Table 1 presents the $\overline{Nu}$ obtained for each grid. We chose the 120×120 non-uniform grid for all the simulations presented in this work.

Table 1: $\overline{Nu}$ for different grids

Mesh	$Ra = 10^6$	$Ra = 1.58 \times 10^9$	$Ra = 4.9 \times 10^{10}$
60×60	8.79709	62.445	171.2870
80×80	8.80758	62.4344	171.2872
100×100	8.81019	62.4204	171.3016
120×120	8.81146	62.4151	171.3080
140×140	8.81258	62.4058	171.3089
160×160	8.81331	62.4015	-

3.2 Flow structure, isotherms and streamlines

Numerical simulations were performed for $Pr = 0.71$, Ra in the range of $10^3 \leq Ra \leq 10^8$ for laminar flow, and two Ra numbers ($Ra = 1.58 \times 10^9$ and $Ra = 4.9 \times 10^{10}$), for turbulent flow. The fluid motion and heating patterns are studied for heated vertical left walls, cooled vertical right walls, and adiabatic top and horizontal surfaces.
Figures 3 and 4 present the isotherms and streamlines for the laminar flow in the range of Ra numbers ($10^3 \leq Ra \leq 10^8$). However, when the Ra is increased, the normal wall temperature gradient increases, and the convection becomes dominant. It is also observed that the center of the cavity becomes more stratified as it can be observed by the isotherms patterns illustrated in Figs. 3(b) through 3(f).

In order to validate the simulations, the results from the present work in terms of average, minimum, and maximum Nu , as well as the position and the maximum velocity into the cavity for the laminar flow are compared with benchmark solutions from the literature.

Table 2 presents the results in terms of average, minimum and maximum Nu as well the position and the maximum velocity in the Ra range ($10^3 \leq Ra \leq 10^6$) obtained in this work and those obtained by Davis (1983). In Tables 2 and 3, columns labeled after 1 denote values obtained in this work, and by 2 denote values from the benchmark solutions. From Table 2, we can see a good agreement between the results for the whole Ra range investigated.

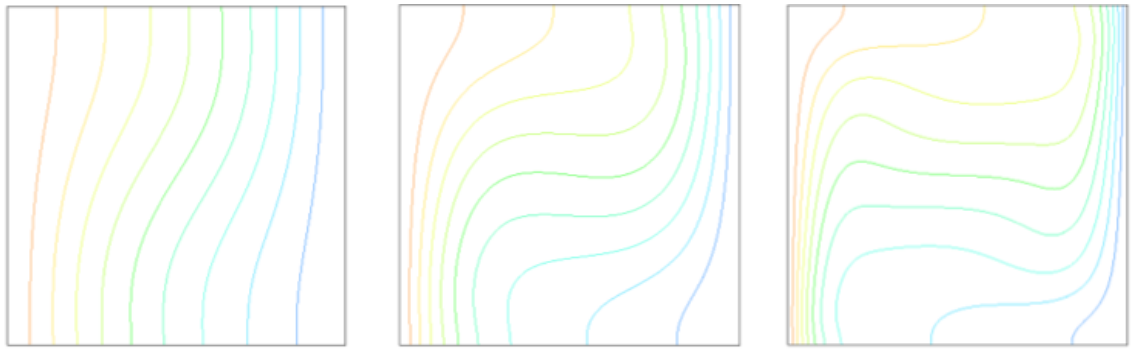

(a) $Ra = 10^3$ (b) $Ra = 10^4$ (c) $Ra = 10^5$

(d) $Ra = 10^6$ (e) $Ra = 10^7$ (f) $Ra = 10^8$

Figure 3: Isotherms for laminar flow.

From the results presented in Table 3, again for laminar regime, we can observe a good agreement between the results

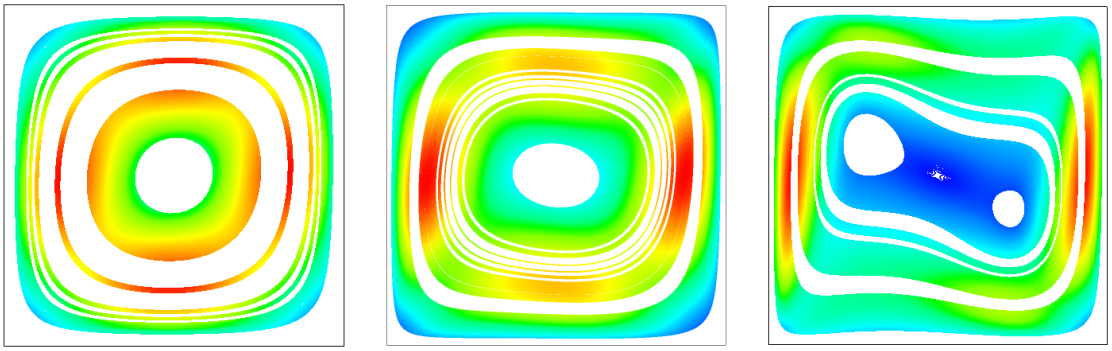

(a) $Ra = 10^3$ (b) $Ra = 10^4$ (c) $Ra = 10^5$

(d) $Ra = 10^6$ (e) $Ra = 10^7$ (f) $Ra = 10^8$

Figure 4: Streamlines for laminar flow

Table 2: Comparison of data for natural convection with those from Davis (1983)

	Ra							
	10^3		10^4		10^5		10^6	
	1	2	1	2	1	2	1	2
V_{max}	3.7	3.697	19.6	19.617	68.6	68.59	220	219.36
X_{max}	0.178	0.178	0.119	0.119	0.0641	0.066	0.038	0.0379
$\overline{Nu}$	1.117	1.118	2.242	2.243	4.515	4.519	8.812	8.799
Nu_{max}	1.51	1.505	3.53	3.528	7.7	7.717	17.5	17.925
Nu_{min}	0.691	0.692	0.585	0.586	0.729	0.729	0.98	0.989

obtained in this work and the ones obtained by Queré (1991).

3.3 Heat transfer rates: Local and Average Nusselt Number

This section presents local Nu number for the whole range ($10^3 \leq Ra \leq 10^8$) of the laminar regime and two values of turbulent regime ($Ra = 1.58 \times 10^9$ and $Ra = 4.9 \times 10^{10}$). We also present the average results for two turbulent regimes investigated.

Figure 5 shows the local Nu along the heated wall. As expected, there is a significant increase in Nu as the Ra increases, due to its convective effects. The heat transfer presents major values in the inferior part of the wall, where occurs the largest temperature gradients. It is also observed that the Nu remain almost constant for small values of Ra number along with the whole length of the wall.

Figure 6 shows the local Nu number along the heated wall for $Ra = 1.58 \times 10^9$. While observing the results in benchmark solution (Table 4), it is noticeable that the Nu in more intern limit layers were not investigated (Ampofo and Karayiannis, 2003). The results are compared with the experimental ones obtained by Ampofo and Karayiannis (2003). Looking closer to the results presented by Ampofo and Karayiannis (2003), it is possible to observe that they did not evaluate the temperature gradients close to lower and upper horizontal walls, where it is expected to be found the higher and lower temperature gradients, respectively. Therefore, is was not possible to compare the numerical results of the present work in these regions. However, for the central part of the cavity a good agreement between the numerical results and those obtained by Ampofo and Karayiannis (2003) was observed.

Table 3: Comparison of data for laminar flow with those from Queré (1991)

	Ra			
	10^7		10^8	
	1	2	1	2
V_{max}	699	699.236	2210	2222.39
X_{max}	0.021	0.021	0.012	0.012
$\overline{Nu}$	16.506	16.523	30.188	30.225
Nu_{max}	39.4	39.3947	86.8	87.2355
Nu_{min}	1.37	1.36635	1.85	1.91907

We present in Fig. 7 the local Nu along the heated wall for $Ra = 4.9 \times 10^{10}$ and the numerical results obtained by Sharif and Liu (2003) using the $k - \omega$ model. From this figure, we can see a good agreement, especially in the regions close to the horizontal walls. As mentioned before, we performed grid refinement study but the results did not change.

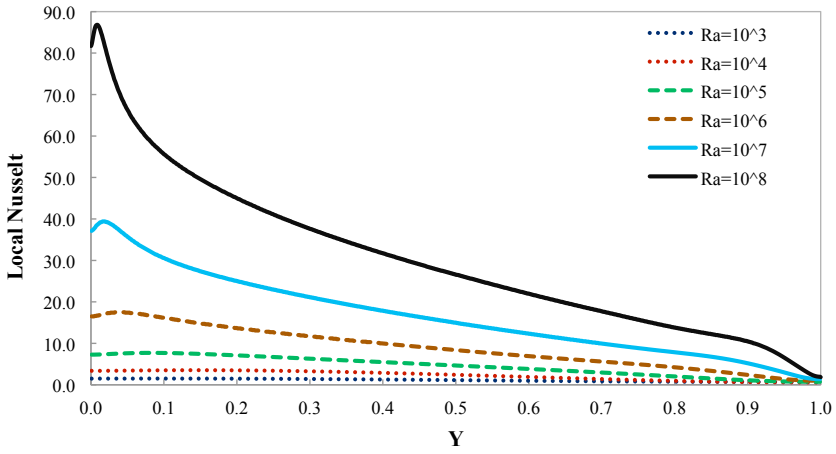

Figure 5: Local Nu along the heated wall for $10^3 \leq Ra \leq 10^8$

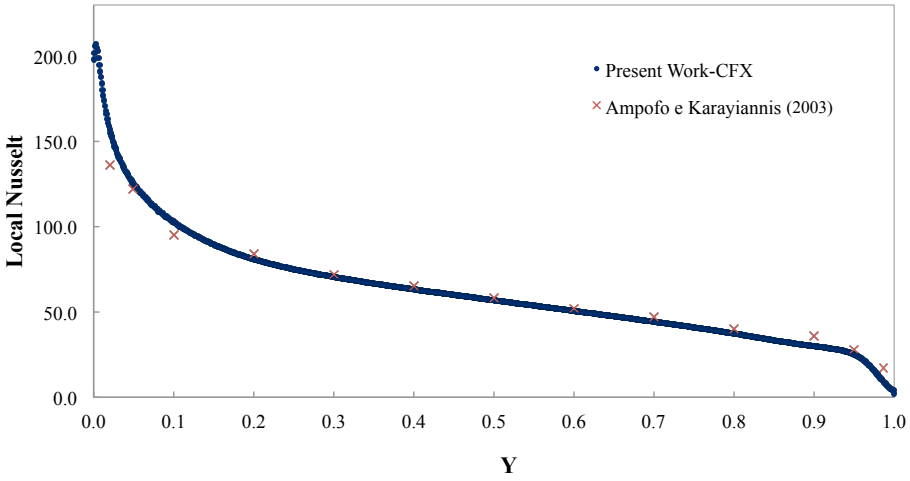

Figure 6: Local Nu along the heated wall for $Ra = 1.58 \times 10^9$

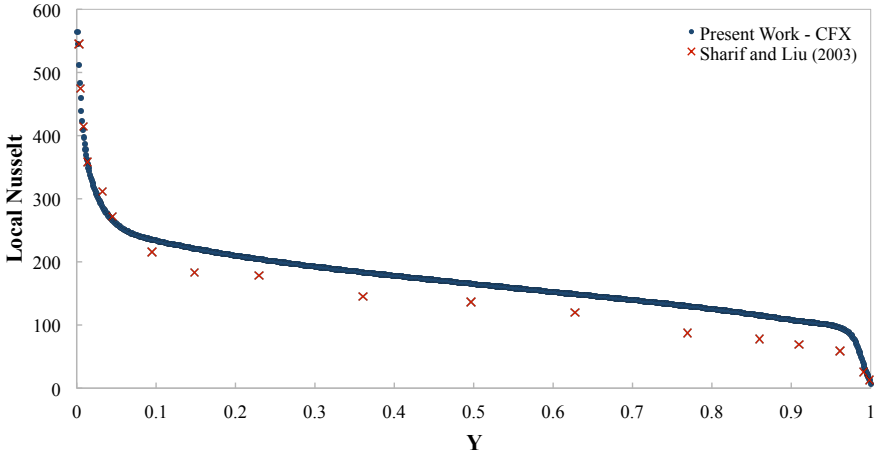

Figure 7: Local Nu along the heated wall for $Ra = 4.9 \times 10^{10}$

Table 4: Comparisons with some Benchmark solutions (Ampofo and Karayiannis, 2003)

$Ra = 1.58 \times 10^9$		
	1	2
V_{max}	0.21	0.2127
X_{max}	0.00501	0.00667
$\overline{Nu}$	62.4	62.9
Nu_{max}	207	136
Y_{max}	0.00314	0.02
Nu_{min}	2.13	17
Y_{min}	1	0.987

4. CONCLUSIONS

The present paper investigated the laminar and turbulent convection in square cavities in the range of $10^3 \leq Ra \leq 4.9 \times 10^{10}$. The $k - \omega$ model was used to model the turbulent regime.The governing equations were solved through the EbFVM (Element based Finite-Volume Method), using the commercial simulator ANSYS CFX®. The results were presented in terms of isotherms, streamlines as well as local and average Nusselt numbers.

For each Ra investigated a mesh refinement was performed, using the average Nu as a parameter. The solution was satisfactory when the variation was lower than $0,1\%$.

The numerical results of the present work were in good agreement with numerical and experimental results available in the literature for laminar and turbulence regime for the natural convection in square cavities. From the numerical results, it was also possible to observe important phenomena such as the boundary layer along the vertical walls, recirculation regions, thermal stratification regions and heat transfer by conduction.

5. REFERENCES

Ampofo, F. and Karayiannis, T.G., 2003. "Experimental benchmark for turbulent natural convection in an air filled square cavity". *International Journal of Heat and Mass Transfer*, Vol. 46, pp. 3551–3572.

Basak, T., Aravind, G. and Roy, S., 2009. "Visualization of heat flow due to natural convection within triangular cavities using Bejan's heatline concept". *International Journal of Heat and Mass Transfer*, Vol. 52, pp. 2824–2833.

Davis, G.V., 1983. "Natural convection of air in a square cavity: a benchmark numerical solution". *Int. J. Num. Methods Fluids*, Vol. 3, pp. 249–264.

Fontana, E., Silva, A.D., Mariani, V.C. and Marcondes, F., 2010. "Numerical investigation of several physical and geometric parameters in the natural convection into trapezoidal cavities". *Numerical Heat Transfer, Part A: Applications*, Vol. 58, pp. 125–145.

Ganguli, A.A., Pandit, A.B. and Joshi, J.B., 2009. "CFD simulation of heat transfer in a two-dimensional vertical enclosure". *Chemical Engineering Research and Design*, Vol. 87, pp. 711–727.

Lam, C.K.G. and Bremhorst, K., 1981. "A modified form of the $k - \epsilon$ model for predicting wall turbulence". *J. Fluids*

Eng., Vol. 103, pp. 456–460.

Lankhorst, A.M., 1991. *Laminar and turbulent natural convection in cavities - numerical modelling and experimental validation*. Ph.D. thesis, Technology University of Delft, The Netherlands.

Queré, P.L., 1991. "Accurate solutions to the square thermally driven cavity at high Rayleigh number". *Int. J. Num. Methods Fluids*, Vol. 20, pp. 29–41.

Rundle, C.A. and Lightstone, M.F., 2007. "Validation of turbulent natural convection in a square cavity for application of CFD modelling to heat transfer and heat flow in atria geometries". In *2nd Canadian Solar Buildings Conference*. Calgary, Canada.

Sharif, M.A.R. and Liu, W., 2003. "Numerical study of turbulent natural convection in a side-heated square cavity at various angles of inclination". *Numerical Heat Transfer, part A: Applications: an International Journal of Computation and Methodology*, Vol. 43:7, pp. 693–716.

Silva, A.D., Fontana, E., Mariani, V.C. and Marcondes, F., 2012. "Numerical investigation of several physical and geometric parameters in the natural convection into trapezoidal cavities". *International Journal of Heat and Mass Transfer*, Vol. 55, pp. 6808–6818.

Trias, F.X., Soria, M., Oliva, A. and Pérez-Segarra, C.D., 2007. "Direct numerical simulations of two and three-dimensional turbulent natural convection flows in a differentially heated cavity of aspect ratio 4". *J. Fluids Mech*, Vol. 586, pp. 259–293.

Vieira, C.B., 2010. *Simulação computacional da convecção natural em cavidades contendo um fluido com geração interna de calor*. Ph.D. thesis, UFRJ/COPPE, programa de energia nuclear, Universidade Federal do Rio de Janeiro, Rio de Janeiro, Brazil.

Wilcox, D.C., 1986. "Multiscale model for turbulent flows". *AIAA 24th Aerospace Sciences Meeting*.